CONCRETE LIBRARY OF JSCE NO. 29, JUNE 1997

EXPERIMENTAL STUDY ON REVERSED LOAD-DISPLACEMENT BEHAVIOR OF RC PIERS USING LARGE-SCALE MODEL

(Translation from Proceeding of JSCE, No. 538/V-31, May 1996)


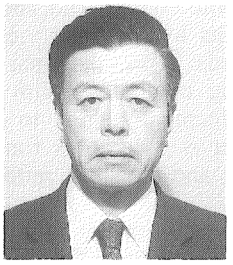
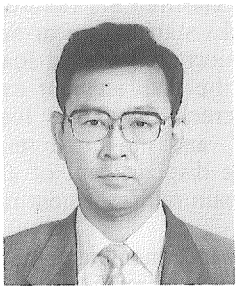
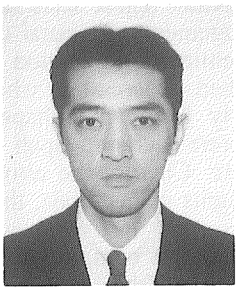

Kenji KOSA Kazuo KOBAYASHI Yasuo MURAYAMA Yoshio YOSHIZAWA

The sectional area of elevated reinforced concrete (RC) bridge piers is generally made small in urban areas because of space constraints. The main reinforcement is then usually multi-layered. In order to evaluate the influence of this multi-layering on the load-displacement behavior of bridge piers, reversed cyclic loading tests were conducted on a large-scale model (1/3 scale) constructed with the same reinforcement details with actual piers as well as on a small-scale model (1/10 scale) for comparison. According to the experimental results, there was no serious decline in ductility in the large-scale model as compared with the small-scale model. However, pull-out of reinforcement from the footings of the large model was three times more serious than in the case of the small model due to the multi-layered arrangement of reinforcement. This suggests that reinforcement pull-out may have a significant influence on the behavior of actual bridges under earthquake loading. On the basis of the bending moment-rotation relationship derived from an analysis of reinforcement pull-out, fiber model based nonlinear RC analysis was conducted on the large scale model with reinforcement pull-out taken into account as rotational spring. It was found that the analytical result was in good agreement with the experimental result.

Keywords: ductility, load-deflection hysteresis, nonlinear analysis, pull-out of reinforcement

---

Kenji Kosa, a member of the JSCE and ASCE, is a senior highway engineer at the Hanshin Expressway Public Corporation, Osaka, Japan. He obtained his Ph.D. from the University of Michigan, Ann Arbor in 1988. His main research interests are the analysis and design of concrete structures.

Kazuo Kobayashi is a professor in the department of Civil Engineering at the Osaka Institute of Technology. He received his Dr. Eng. from Kyoto University in 1973. He has authored several books and a number of technical papers in the analysis and design of reinforced and prestressed concrete structures. He is a member of the JSCE.

Yasuo Murayama is a senior manager at the Technical Research Institute in Kajima Corporation. He obtained his Dr. Eng. from Kyushu University in 1995. He is a registered engineer and a member of the JSCE and JCI. His main research interest is the seismic design of concrete structures.

Yoshio Yoshizawa is a chief at CTI Engineering Co., Ltd. He obtained his BS in civil engineering from Saitama University in 1986. His research interest is the design of concrete structures. He is a registered consulting engineer and a member of the JSCE.

---

1. INTRODUCTION

In earthquake-prone countries like Japan, the reinforcement details of RC bridge piers are predominantly determined by the seismic load because seismic resistance is of such importance. To date, a number of reversed loading tests have been carried out on the behavior of RC piers under seismic loading by investigators such as Akimoto[1], Kawashima [2], Ishibashi [3], Osaka[4], and Machida[5]. These tests have clarified the failure pattern of piers with a conventional reinforcement arrangement. Flexural cracks start to appear near the column end and they gradually spread over the entire cross section subject to reversed loadings by the time yielding displacement (δ_y) is reached. Thereafter, when the displacement exceeds 2 δ_y, diagonal cracks begin to occur and slowly form an x-shaped crack pattern as loading continues. With further advance, the cover concrete starts to spall off, and the main reinforcement begins to buckle, leading to ultimate failure. Clearly, the ultimate displacement of a pier is a complex function of such factors as the strengths of materials, the main reinforcement ratio, and the shear reinforcement ratio.

Despite this complexity, the specimens used in past experiments have been to 1/6 scale at most, as shown in Table 1, due to various restrictions associated with the experiments, typically cost and experimental complexity. They are roughly 50 cm in width and simulate the cross section of real piers only by the reinforcement ratio.

However, given the failure process mentioned above, it is clear that the arrangement of reinforcement plays a crucial role in the behavior of RC piers in the ultimate state. For example, it has been pointed out that if a small specimen, 10 x 10 cm, with only one reinforcing bar in each corner is used in an experiment, a significant decline in load bearing capacity occurs as soon as core concrete has been damaged, and thus the derived results do in fact differ from the behavior of an actual bridge in its ultimate state[2]. Also, the degree of influence of reinforcement pull-out from the footing on the overall horizontal deformation, which is approximately 50% in small specimens, is generally considered substantially less in the case of real piers, because the reinforcement diameter in real piers is typically small compared with the cross-sectional size of the column.
However, few studies have attempted to consider this issue on the real bridge level. Further, in the case of elevated bridge piers in urban areas, it is feared that the ultimate bearing capacity may be further decreased and reinforcement pull-out further increased under loading because they contain a large amount of reinforcement to compensate for their slim configuration compared with ordinary piers. To summarize, the reinforcement details of ordinary small specimens differ from those in urban elevated bridge piers in the following points:

Table 1 Reverse-loading testes in the literature

investigators	dimensions (cm) and the number of specimens	main parameters
Kawashima et al.	40×80×240 : 25 50×50×240~250 : 15	main reinforcement ratio, loading type, hoop tie ratio, concrete strength, bending moment / shear force ratio
Yamamoto et al.	35×150×100~200 : 12 60×60×130 : 4 40×60×95~155 : 5 ϕ65×165~230 : 6	bending moment / shear force ratio, tension reinforcement ratio, axial stress, shear reinforcement ratio
Osaka et al.	40×40×140 : 12	main reinforcement ratio, hoop tie ratio, axial stress
Machida et al.	20×15×85 : 33	bending moment / shear force ratio, tension reinforcement ratio, axial stress, hoop tie ratio, concrete strength
Ishibashi et al.	40×40×150 : 27 40×50×115 : 15 60×40×150 : 4	tension reinforcement ratio, hoop tie ratio,axial stress, concrete strength

① The diameter of the reinforcement in small specimens is relatively large compared with the column dimensions.
② The main reinforcement is single-layered in small specimens, whereas in real piers it is multi-layered.
③ The main reinforcement is not cut off at the midheight of the column, whereas in real piers it is cut off at the midheight.
④ Hoop ties are closed in the cross section of small specimens, but they are not closed in real piers.

These disparities may cause a difference in the ultimate displacement and ductility between small test specimens and real piers. Hence, in our experiment aimed at reproducing the behavior of real piers as closely as possible, a large size model (1/3 scale of column-end flexural failure type) was constructed with reinforcement details identical to those of elevated bridge piers used in urban areas. Cyclic loading was applied at the column top in the horizontal direction and the test results were compared with those obtained with a small specimen (1/10 scale). Next, in order to quantitatively evaluate the reinforcement pull-out due to the effect of the multi-layered reinforcement arrangement, reinforcement stress-pull out analysis was conducted using a bond-slip hysteresis model proposed by Suzuki et al. [6] as well as a stress-strain model. Then, to evaluate the overall behavior of the specimen subjected to loading, a P- δ simulation analysis was carried out based on the nonlinear RC analysis method using a fiber model and taking into account reinforcement pull-out from the footing as a nonlinear rotation spring. Through this procedure, a modeling method for successfully predicting the load-deformation behavior of real bridge piers under seismic loading is proposed.

2. EXPERIMENTAL PROCEDURE

2.1 Specimen preparation

a) Configuration and reinforcement details
Two specimens were prepared: one small and the other large. The dimensions of the large specimen and the test set-up are shown in Fig. 1. The cross-sectional reinforcement details of the

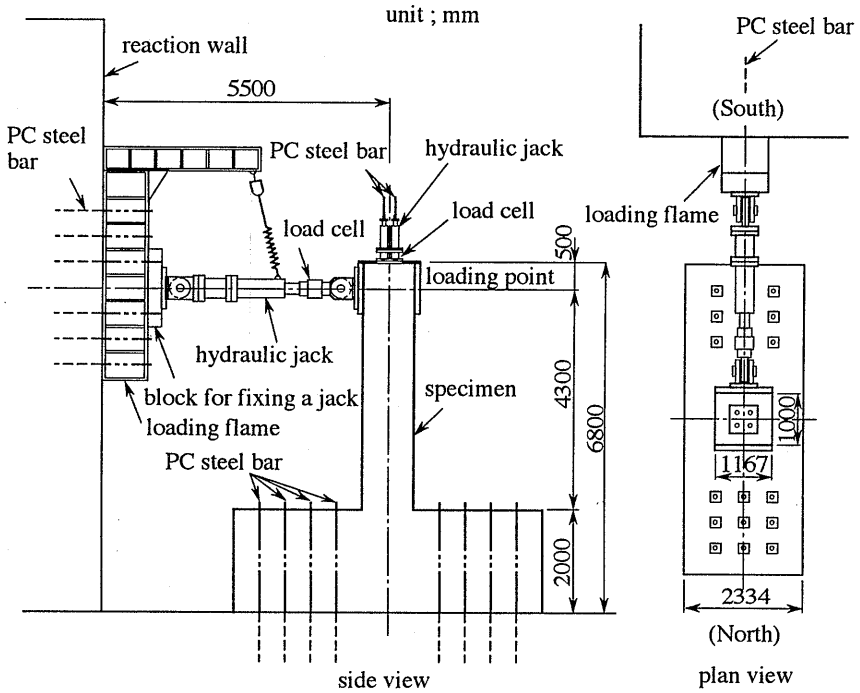

Fig. 1 Dimensions of the specimen and loading method (Large size model)

two specimens are shown in Fig. 2. The shear span ratio of the column (a/d, a: shear span length, d: cross sectional size in the direction of applied loading) was 4.3, the main reinforcement ratio (the ratio of cross sectional areas of main reinforcement and column) was 2.2% and the hoop tie ratio was 0.3% at the column end in both specimens.

The small specimen (1/10 scale), manufactured with a similar shape and the same reinforcement ratio as the large specimen, was used for comparisons with the large specimen. Relatively large diameter reinforcing bars compared with the column cross section were used in the small specimen: D19 bars as the main reinforcement and D6 as the hoop ties.

The large specimen was a 1/3 scale model manufactured to model the reinforcement details of a real pier. In a real pier, D35 and D19 bars are commonly used as the main reinforcement and hoop ties, respectively. In this large model, D13 and D6 bars were used, respectively, in accordance with the reduced scale of the specimen as compared with a real pier. The main reinforcing bars were arranged in three layers in the lower section of the column, and the inner-most layer was extended up to a point 2.16 m above the upper face of the footings. This position was determined by adding the effective depth of the column cross section to the point at which such cut-off is allowed by calculation according to the Japanese Specifications for Highway Bridges.

Main reinforcement was extended down to the bottom face of the footing and anchored there. The spacing of the main reinforcement was 7.6 ϕ (ϕ : reinforcement diameter) in the small specimen, whereas in the large specimen the spacing between bars was 3.6 ϕ and the spacing between layers was 2.6 ϕ. As to the shape of the hoop ties, a closed type with hooks at both ends was used in the small specimen, whereas in the large specimen hoop ties bent into a U shape in compliance with those used in real piers were inserted from both sides and closed with lap splices. As shown in Fig. 2, intermediate hoops were placed in a proportion of 0.1% in terms of hoop tie ratio.

b) Materials

The mechanical properties of the reinforcement such as yield point, tensile strength, and strain hardening point were identical in both specimens, as seen in Table 2. High-early-strength Portland cement was used for concrete. In the small specimen, ready-mixed concrete with a maximum aggregate size G_{max} of 20mm was used, whereas in the large specimen, " micro concrete " with G_{max} =10 mm was used in consideration of the reduced scale of the specimen compared with a real pier. The mix proportion of the concrete and its strength at the time of loading tests are shown in Tables 3 and 4, respectively.

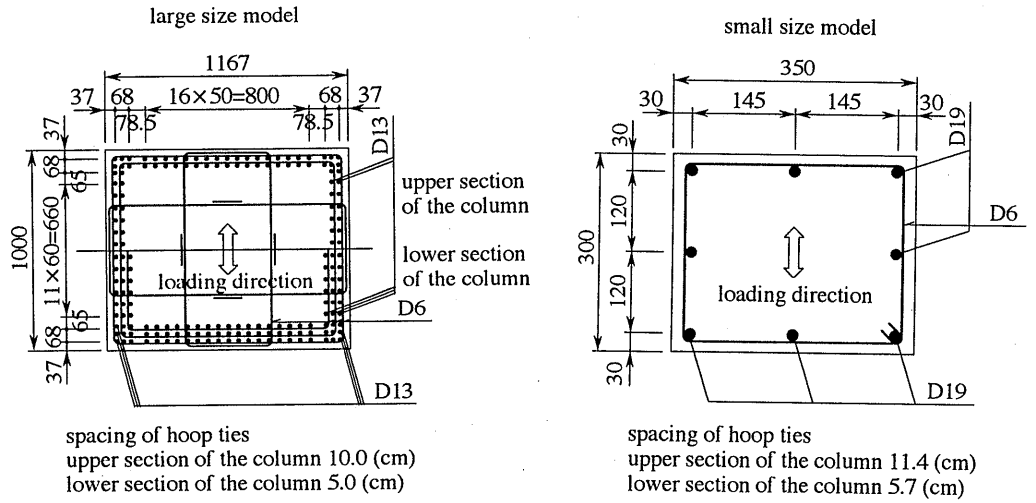

Fig. 2 Cross sectional size and reinforcement details

2.2 Loading and measurements

Loading was applied to the column top in a horizontal direction while the column was subject to an axial force from the top so that the axial stress acting on a real pier was taken into account. The loading set-up is shown in Fig. 1. An axial force equivalent to a stress of 15kgf/cm ^{2} was applied using a jack fitted to the column top via a prestressing steel bar through the center of the specimen and anchored at the footings. This steel bar was encased in a sheath of such size that the bar did not touch it even when the specimen was deformed.

In both specimens, incremental reverse loading was applied by load control method up to the yield load P_y determined by calculation. This P_y is the load at which the outer-most main reinforcement around the column end reaches the yield point. After the yield load was reached, 10 cycles of reversed loading with the same displacement amplitude were applied successively at multiples of δ_y. Loading was continued by the displacement control method until the load fell to the yield value after reaching the maximum load. The yield load P_y and the corresponding displacement δ_y were 8.5 tf and 10.5 mm in the small specimen, and 92 tf and 26 mm in the large specimen.

Table 2 Properties of reinforcements used

	diameter	yield point (kgf/mm^2)	tensile strength (kgf/mm^2)	strain hardening (%)	elongation (%)	contraction (%)
main reinforcements of large specimen	D13	38.3	57.1	1.7	26	48
main reinforcements of small specimen	D19	39.1	57.7	1.5	23	42
hoop ties	D6	32.6	44.2	3.0	16	57

Table 3 Mix proportion of concrete

	max. size of coarse aggregates (mm)	slump (cm)	air content (%)	water/cement ratio (w/c) (%)	ratio of fine aggregates S/a (%)	unit content (kg/m^3) water W	cement C	fine aggregates S	coarse aggregates G	admixture
large model	10	18	4	62.0	46.0	200	323	785	951	0.808
small model	20	15	4	57.5	44.8	175	305	801	1015	0.762

Table 4 Concrete strength at the time of experiment

	compressive strength (kgf/cm^2)	tensile strength (kgf/cm^2)	Young's modulus ($\times 10^6$ kgf/cm^2)
large model	283	24	0.22
small model	278	26	0.29

Measurements included displacement at the loading point, the distribution of horizontal displacement in the longitudinal direction, the relative vertical displacement of the footings and the column, and the strain of main reinforcement in the footings, as shown in Fig. 3.

3. EXPERIMENTAL RESULTS AND DISCUSSION

3.1 Results for small specimen

Load-displacement hysteresis loops for the two specimens obtained at multiples of δ_y are shown in Fig. 4. The distribution of horizontal displacement in the longitudinal direction at each displacement step is given in Fig. 5, and the crack and failure conditions are shown in Fig. 6. As seen from Fig. 4, the load-displacement envelope (P - δ) indicates that a maximum load of 11.2 tf was reached at a displacement of 4 δ_y, and that the capacity did not visibly decrease even when a displacement of 5 δ_y was reached. The yield ratio, which is the ratio of yield load to maximum load, was approximately 0.75.

Regarding the displacement ductility factor, several definitions have been proposed: one, for example, takes the ductility factor at the point when the load falls to the yield load after reaching the maximum load; another takes the ductility factor at the point when the load falls to 80% of the maximum load. In our experiment, however, since the yield ratio was 0.75, the ductility factor was roughly identical whichever definition was adopted. The resulting displacement ductility factor, slightly smaller than 6, is 1.2 times bigger than the value calculated using the equation proposed by Machida et al. (based on the latter definition) [5] . Nevertheless, given the 20% scatter in their experimental results, it can be considered that our test on the small specimen basically differs little from past experiments by other investigators.

3.2 Results for large specimen

The shape of the load-displacement envelope (P - δ) for the large specimen is roughly identical to that of the small specimen, as seen in Fig. 4. The maximum load of the large specimen was 122 tf, whereas that of the small specimen was 11.2 tf. This difference is approximately the second power of the size difference between the two specimens. The ductility factor was roughly 5.5, slightly smaller than but broadly similar to the ductility factor of the small specimen.

Though diagonal cracks appeared from the early loading stage around the point where the main reinforcement was cut off, this section did not undergo yielding or indicate damage progress even when the maximum load was reached. As a result, the distribution of displacement at over 3 δy was roughly linear, as seen in Fig. 5, implying that the main cause of deformation is concentrated in the area around the fixed end of the column. This was also the case with the small specimen. However, looking at the yielding displacement (1 δ_y) , it is somewhat smaller than the value obtained by scaling up in accordance with the size difference between the two specimens. Also, several portions of the main reinforcement ruptured while cyclic loading was being applied with a displacement of 5 δ_y , a behavior not observed in the small specimen test.

3.3 Discussion

As described above, the deformation behavior was roughly the same for both specimens, but there were minor differences. The following discussion focuses on the potentially influential factors mentioned earlier.

a) Effect of main reinforcement cut-off
In the large specimen, the yield ratio was 0.75, whereas the ratio of the distance between loading point and cut-off point vs. shear span length was about 0.5. Hence, the specimen had been given a considerably large safety factor, approximately 1.5 by calculation, and so no yielding was observed in the area of the main reinforcement cut-off. Since the displacement observed at the column top in the large deformation stage was mostly a result of plastic deformation at the

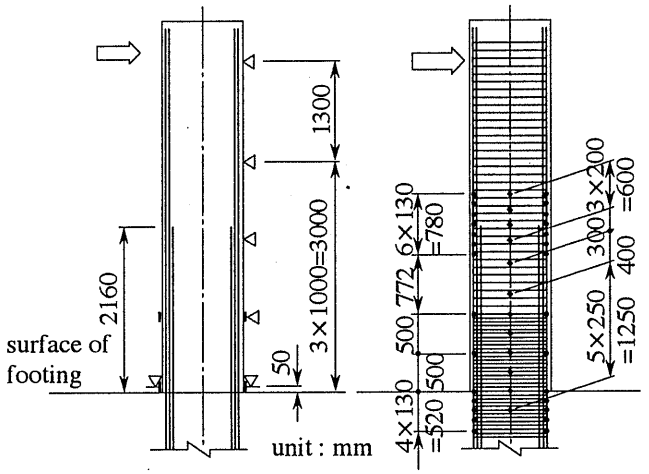

△ : LVDT
▮ : concrete strain gauge
● : main reinforcement strain gauge
◆ : hoop tie strain gauge

Fig. 3 Measuring points

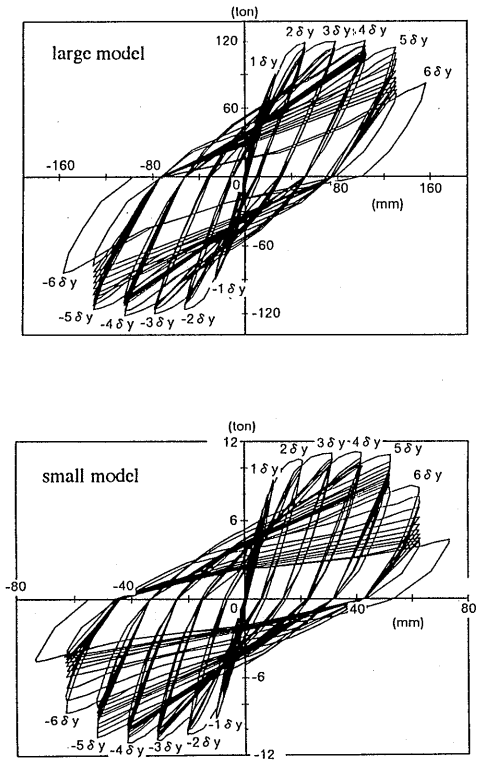

Fig. 4 Load-displacement hysteresis loops at loading points

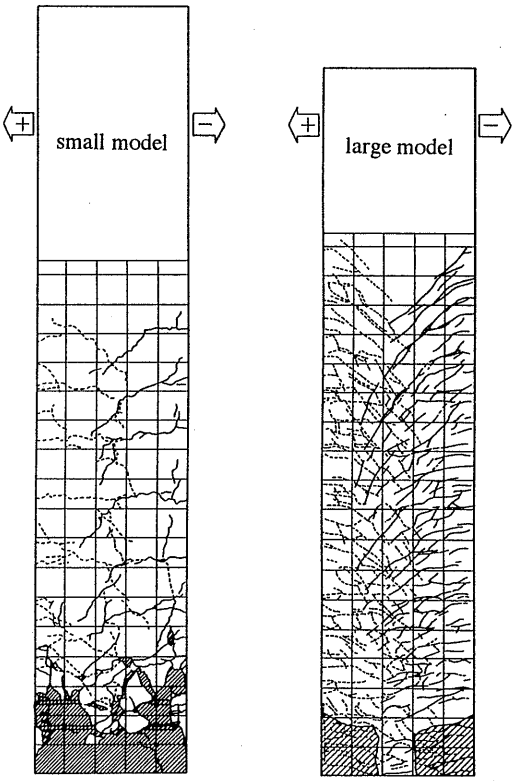

Fig. 6 Crack and failure conditions

column end as well as by deformation associated with pull-out of the main reinforcement at the footing, it can be concluded that the effect of main reinforcement cut-off on the overall deformation of real piers will remain very minor if the cut-off point is determined as in this case.

b) Effect of multi-layered arrangement of reinforcement
The distribution of the main reinforcement strain in the longitudinal direction in the area below the cut-off point was roughly similar in both large and small specimens. However, in the large size specimen, the reinforcement showed a longer yield extension in the footing as illustrated in Fig. 7 and the reinforcement stress was transferred deep into the footings. As a result, as shown in Fig. 8, the amount of main reinforcement pull-out from the footing is consistently greater in the large specimen made of D13 bars than in the small specimen containing D19 bars when compared at the same ductility ratio.

When reinforcement pull-out is compared at 4 δ_y, close to the ultimate displacement, in terms of a non-dimensional reinforcement diameter, it is 0.4 ϕ in the large specimen, approximately three times bigger than the 0.13 ϕ of the small specimen. This is because the spacing of the main reinforcement in the large specimen (3.8 ϕ , 2.6 ϕ) is closer than that of the small specimen (7.8 ϕ). The value (0.4 ϕ) is, however, considerably larger than the 0.2 ϕ derived by Ishibashi et al. [3] . This is probably because the bond strength between each bar and concrete decreases due to the multi-layered arrangement of the reinforcement.

The ratio of column top displacement caused by column end rotation to overall displacement was small in the large specimen compared with that of the small specimen, as shown in Fig. 9. The loops shown in Fig. 9 are similar to the results of existing studies by others. However, given that our data shows about 25% of the ultimate displacement at the column top being attributed to rotation at the column end, the effect of reinforcement pull-out in actual piers cannot necessarily be assumed to remain minor.

c) Effects of reinforcement diameter and the shape of hoop ties
In the small specimen, fracture occurred in the column in the range 0.8d from the column end, which is roughly similar to the results by other investigators. In contrast, in the large specimen, it occurred in the range 0.4d from the column end (Fig. 6). According to visual observations, the length of the fracture region in both specimens roughly corresponded with the region in which the main reinforcement buckled. The difference in the fracture range (0.8d vs. 0.4d) is considered attributable to differences in main reinforcement diameter and the shape and size of the hoop ties used. The cause of main reinforcement rupture in the large specimen is possibly that fracturing was concentrated excessively in a narrow range around the column end. In the large specimen, the lap-spliced hoop ties were reinforced by intermediate hoops amounting to 0.1% in terms of hoop tie ratio in the same way as done in real piers.

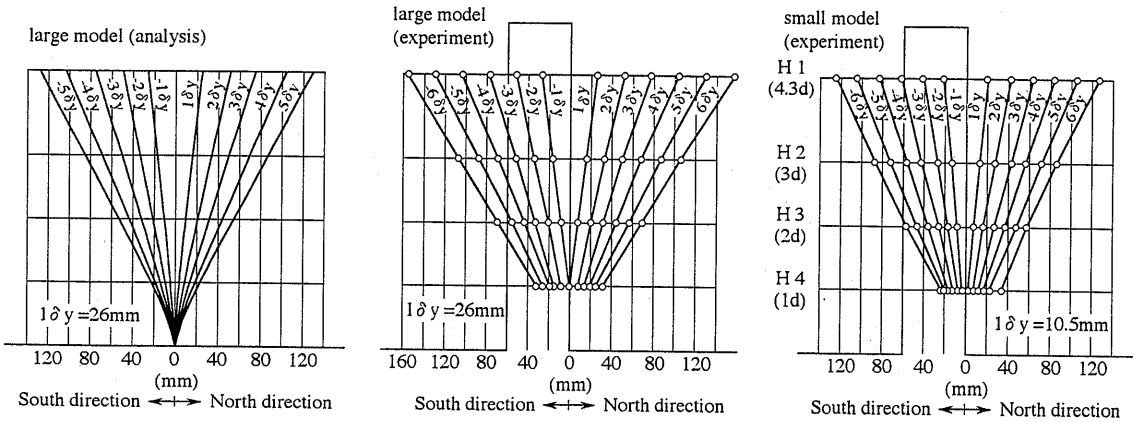

Fig. 5 Distribution of horizontal displacement in the longitudinal direction

The strain of the intermediate hoop measured on the plane perpendicular to the loaded plane was quantitatively similar to the hoop tie strain. Accordingly, it is concluded that intermediate hoops performed as expected as shear reinforcement. Also, in the case of the large specimen, it is inferred that the presence of the intermediate hoops restrains the decrease of confinement due to the enlargement of hoop ties, and that a deformation capacity no different from that of the small specimen was achieved as a result.

4. ANALYTICAL INVESTIGATION OF MAIN REINFORCEMENT PULL-OUT

4.1 Outline

Conventionally, it has been accepted that the influence of rotation at the column end due to main reinforcement pull-out on displacement at the column top, and consequently on the overall deformation capacity, is large in small specimens, but that it is comparatively small in real piers. However, our experiment on the large specimen indicates that this influence is not necessarily small, because the bond strength between concrete and reinforcement degrades in elevated bridge piers designed for urban use due to the close arrangement of main reinforcement. To evaluate this effect analytically, a numerical investigation was carried out on the amount of reinforcement pull-out from the footing in the large specimen.

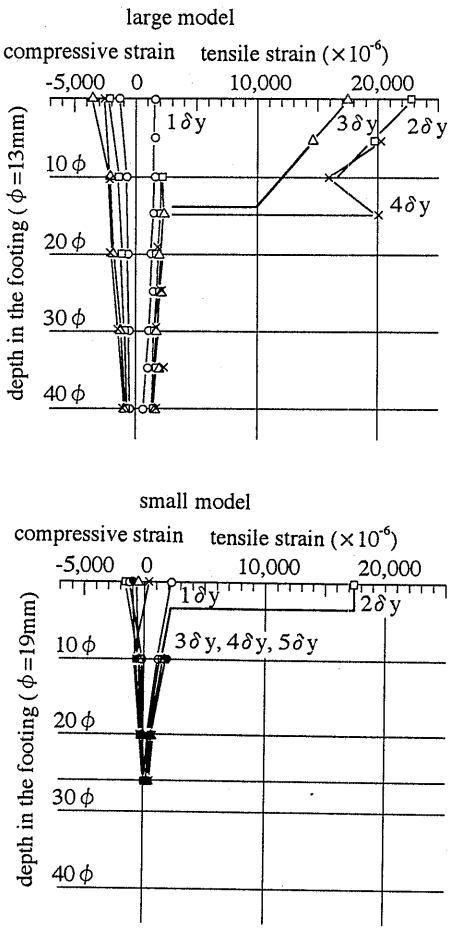

Fig. 7 Distribution of main reinforcement strain in the footing

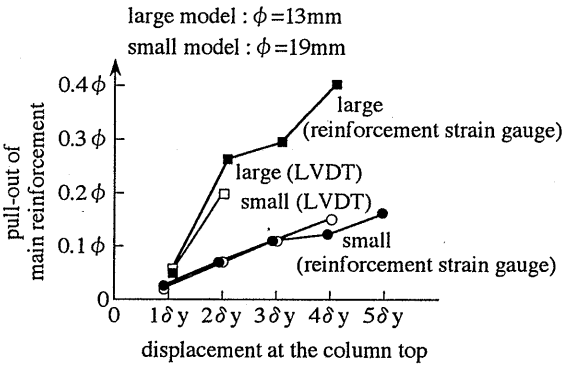

Fig. 8 The relationship between pull-out of main reinforcement and displacement

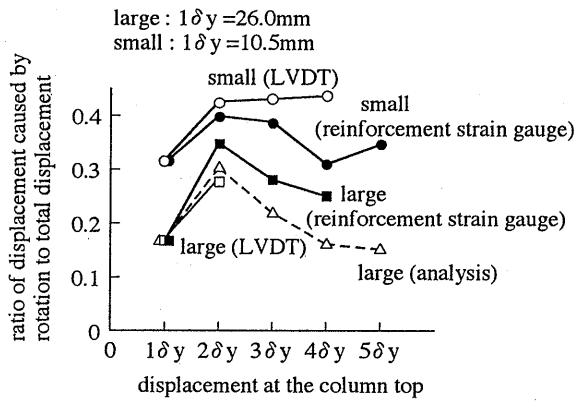

Fig. 9 Ratio of displacement caused by rotation to total displacement at the column top

4.2 Method of analysis

Analysis associated with reinforcement pull-out is often conducted using a stress-strain relationship for the reinforcement ($\sigma - \varepsilon$ model) and a bond-slip relationship between the reinforcement and concrete (τ - s model). This procedure was employed in our analysis. The Menegotto-Pinto model [12] was used as the $\sigma - \varepsilon$ relationship. This model is characterized by the explicit derivation of stress level from reinforcement strain. As the τ - s model, the model shown in Fig. 10 as proposed by Suzuki et al. [6] for the analysis of main reinforcement pull-out was used.

4.3 Results of analysis

Analysis was conducted on the reinforcement pull-out from the footing. The strain distribution of main reinforcement in the footing was calculated under conditions that the analytical reinforcement stress was in conformity with the measured stress up to yielding and, after that the analytical reinforcement pull-out expressed by an integral of reinforcement strain was in conformity with the measured stress. The calculated strain distribution is compared with the experimental result in Fig. 11.

The calculation agrees well with the experimental result in the case of the small specimen. With regard to development length (the distance from the upper face of the footing to the position where the reinforcement strain reaches almost zero), the calculation is roughly in agreement with the experimental result. In particular, the calculation fairly successfully expresses the yielding range of reinforcement near the face of the footing at a displacement of 2 δ_y. In contrast, in the case of the large specimen, the calculation failed to estimate the experimental result as good as in the case of the small specimen. Although both calculation and experimental results are similar in terms of the pattern of yielding zone, they deviate quantitatively. Also, strain of the elastic zone are in a 'shallow' range in the calculation, a different tendency from the experiment. It can be said that this is because the bond strength is lower in the large specimen due to the dense arrangement of bars, whereas the proposed τ - s model is intended for columns with relatively large reinforcement spacing.

4.4 Modification of analytical bond-slip model

The τ - s model shown in Fig. 10 was modified so as to reflect the influence of the closer reinforcement spacing in the large specimen. The modifications are outlined below.

① Change the amount of yielding slip (S_y) of 0.014 ϕ derived from the τ - s model by Suzuki et al. to 0.08 ϕ based on the experimental result.
② Reduce the bond strength, or change the scale of the τ axis, to take into account the influence of reinforcement spacing as suggested by Ishibashi et al. [3]
③ As a reduction coefficient for the bond strength influenced by the reinforcement spacing, adopt the product of the reduction coefficient due to the spacing between layers and the reduction coefficient due to the spacing between main reinforcement bars. The reduction coefficient calculated in this way is approximately 30% for the large specimen.
④ Adjust the residual constant bond strength (τ_R) after yielding to match the calculated pull-out after yielding with the experiment.

The modified τ - s model thus established is shown in Fig. 12. Indicated in Fig. 13 are the calculated strain distribution corresponding to the measured reinforcement pull-out derived using the modified τ -s model. From this figure, it is clear that the strain distribution in the large specimen associated with pull-out of the main reinforcement is well predicted when the modified τ -s model is adopted.

4.5 Analysis of M- θ hysteresis loop at the column end

Using the modified τ -s model, the bending moment-pull out hysteresis loop was calculated.

Next, using this result, the hysteresis loop for the bending moment-rotation angle (M- θ) at the fixed end due to pull-out was calculated. To derive the θ value, hysteresis values for reinforcement stress and position of the neutral axis are needed. For this purpose, the relationships between bending moment and reinforcement stress, and between bending moment and the neural axis at the column end were calculated in advance by the fiber model based analysis. The analytical M- θ hysteresis loop is compared in Fig. 14 with the measured result. The measured hysteresis loop was obtained from the relative vertical displacement between footings and column taken on the two opposite sides. As seen from the figure, the measured M- θ hysteresis loop shows a pattern similar to that of the P- δ curve, which indicates that analytical result is able to predict the measured M- θ loop up to roughly a displacement of 3 δ_y.

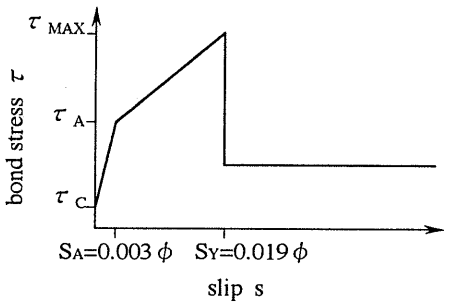

Fig. 10 τ - s model

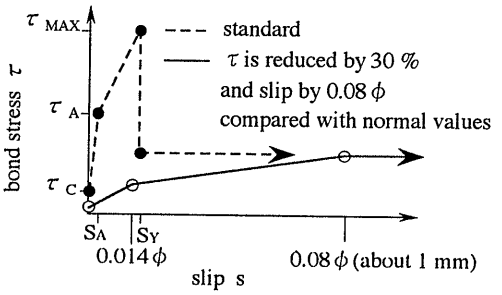

Fig. 12 Modified τ - s model

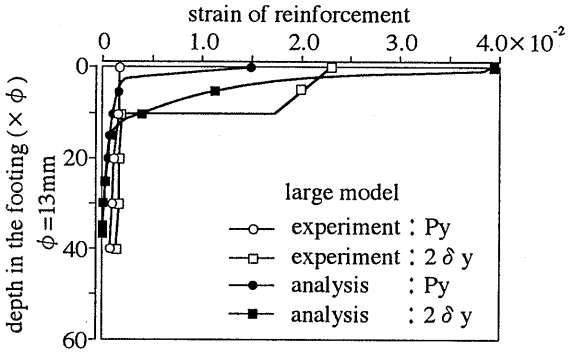

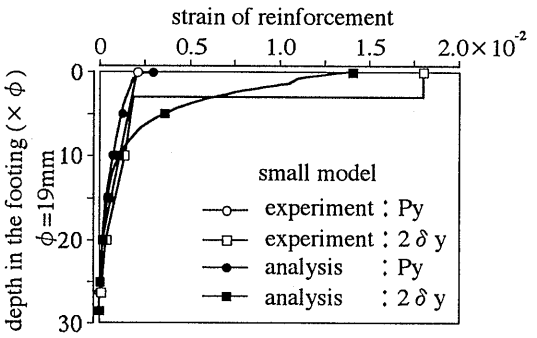

Fig. 11 Distribution of reinforcement strain in the axial direction

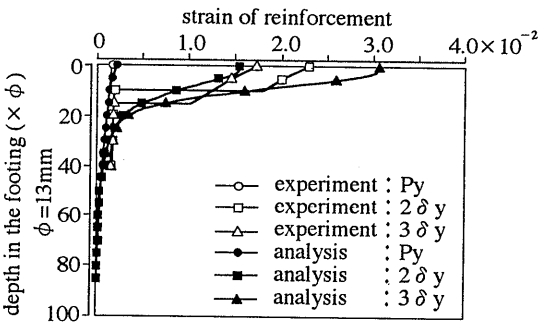

Fig. 13 Reinforcement strain in the axial direction (Large model)

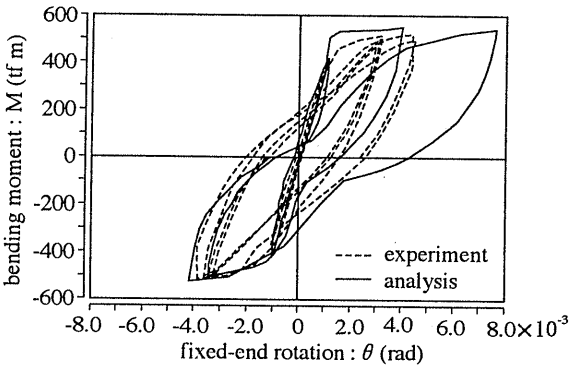

Fig. 14 M- θ hysteresis loop

5. ANALYTICAL INVESTIGATION OF THE P- δ CURVE OF THE COLUMN

5.1 Outline

One effective method of estimating the ultimate resistivity of bridges against strong earthquake loading is to carry out nonlinear seismic response analysis. In doing so, it is important that the nonlinear hysteresis characteristics of the structural members constituting the bridge should be reflected accurately in the analysis. This is particularly important in a pier where the design is governed by seismic loading. Accordingly, in our study, analytical investigation was conducted on the large model that simulated the influence of rotation at the column end due to pull out of main reinforcement.

The fiber model based analysis was employed for the analysis. This method assumes that the column comprises multiple bar members and that the column cross section is constituted of elements of concrete and reinforcement. It also presumes that the cross section remains plane after deformation and that the material properties are those under the uniaxial stress state. This method is advantageous in that it is applicable to a wide range of cross sectional features, material properties, and loading conditions compared with a method using empirical load-displacement hysteresis models. Also, the labor and time needed for calculation are significantly less than for FEM analysis.

5.2 Modeling of the column member

a) Material models
As the material models, those used by Yamada et al. [10] were employed. Namely, the concrete is modeled using the $\sigma_c - \varepsilon_c$ hysteresis loop based on the rule by Muguruma et al. [11]. As for the reinforcement, the $\sigma_s - \varepsilon_s$ hysteresis loop proposed by Menegotto-Pinto [12] was utilized. The concrete model and the reinforcement model are shown in Fig. 15 and Fig. 16, respectively. The physical properties of the materials used are given in Table 5.

b) Modeling of the member and cross section
As shown in Fig. 17, the column member was divided into a total of 19 elements in the longitudinal direction. Elements in the possible plastic region in the range up to 1.0 m from the column end were made small. The cross section was divided into 50 fibers and reinforcement elements were taken into account according to the arrangement of bars at each position along the column.

5.3 Model for the rotation spring at the column end

A rotation spring was installed at the column end, in which a series model of the linear spring and nonlinear hysteresis spring was taken into account. The linear spring and the nonlinear hysteresis spring take into account elastic deformation of the footing and the pull-out of the main reinforcement, respectively. By placing these springs in series, the displacement is determined as the sum of the displacements of each spring when a bending moment acts on the column end.

a) Linear spring
The linear spring was established by taking into consideration the difference between Young's modulus of the concrete model and that of the micro concrete, the shear deformation of the column, and the deformation of the footings.

b) Nonlinear hysteresis spring
The trilinear model shown in Fig. 18, as proposed by Muto, was used as the nonlinear rotation spring at the column end. The characteristics of the skeleton curve were determined with reference to measured and analytical results of the M- θ hysteresis loop: 4.7×10^5 tfm/rad for the first gradient; 2.1×10^5 tfm/rad for the second gradient; and 1.8×10^4 tfm/rad for the third gradient. The rotation angles at the two inflection points were made 6×10^{-4} rad and 1.5×10^{-3} rad.

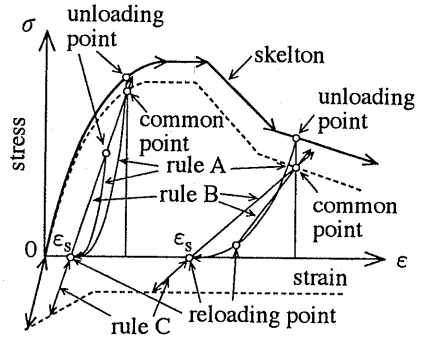

Fig. 15 Model for the stress-strain relationship of concrete

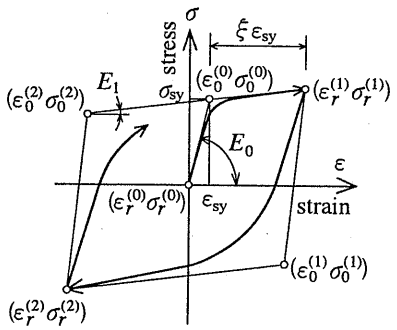

Fig. 16 Model for the stress-strain relationship of reinforcement

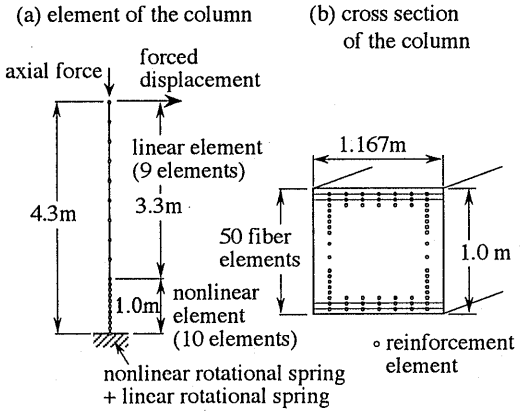

Fig. 17 Analytical model for the column

Table 5 Physical properties (unit : kgf/cm²)

Young's modulus of concrete	2.2×10^5
compressive strength	283
Young's modulus of reinforcement	2.1×10^6
yield strength	3830
second gradient	4.2×10^4

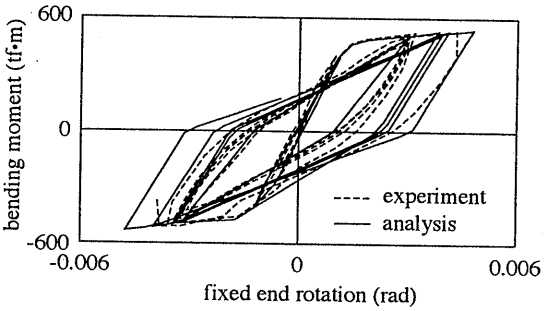

Fig. 18 Relationship of bending moment-rotation at the column end

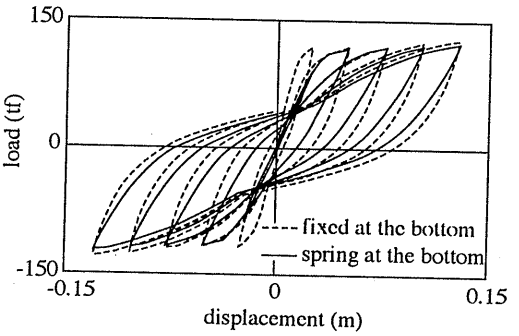

Fig. 19 Relationship of load-displacement at loading points

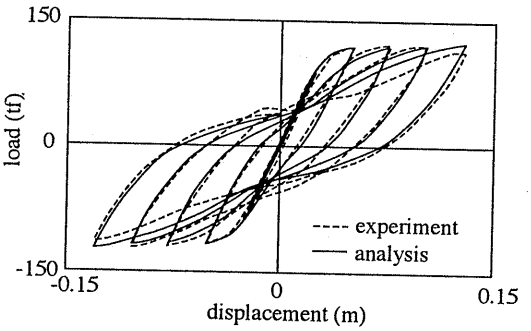

Fig. 20 Comparison of experimental and analytical results on load-displacement relationship

Analytical results of the P - δ hysteresis loop at the column top are shown in Fig. 19. Two cases are compared: one ignores the rotation spring at the column end and the other takes it into account. The analytical result for the case where the rotation spring is considered is compared in Fig. 20 with the experimental result. The analytical M- θ loop at the column end due to pull-out is compared in Fig. 18 with the experimental result. The proportion of the displacement at the column top attributed to rotation at the column end induced by the reinforcement pull-out as a ratio of overall displacement at the column top is given in Fig. 9. The distribution of horizontal displacement along the column in the longitudinal direction is shown in Fig. 5.

From these figures, it is found that a larger load is given by calculations with the same plastic factor when the rotation spring is ignored (which means that the column end is fixed) compared with when it is taken into consideration; this is because the rigidity of the member as a whole is increased in the former case. This tendency is particularly conspicuous at the time of 1 δ_y (Fig. 19). In contrast, if the rotation spring is taken into account, it is possible to estimate the skeleton of the P - δ curve and the hysteresis loop with better accuracy (Fig. 20).

The analytical M- θ loop is in relatively good agreement with the experimental result, which suggests that the Muto model is adequate for the analysis of the rotation spring at the column end in relation to reinforcement pull-out (Fig. 18). In the analytical result, the proportion of displacement at the column top attributed to rotation at the column end is approximately 20% at 1 δ_y and 30% at 2 δ_y. These values are close to those obtained in the experiment (Fig. 9). In the analysis, the proportion of displacement at the column top attributable to rotation of the column end decreased near the ultimate state compared with the proportion at 2 δ_y or 3 δ_y. For example, it was 15% at the displacement of 4 δ_y (Fig. 9).

The distribution of horizontal displacement in the longitudinal direction was roughly linear in the analytical result, except in the area around the column end, and this is in good agreement with the experimental result, which showed that the bulk of displacement at the column top is governed by deformation around the column end (Fig. 5).

6. CONCLUSIONS

Experimental and analytical investigations were conducted using a large model (1/3 scale) constructed with the reinforcement arrangement of a real pier as well as with a small model (1/10 scale). The type of RC bridge piers used in urban areas was adopted as the prototype. The following conclusions can be drawn from the results:

① The P- δ envelope obtained in the experiment on the large model was roughly identical to that obtained from the small model. The displacement ductility factor of the large model was 5.5, which was slightly smaller than that of the small model, which was 6.0.

② The amount of reinforcement pull-out in the large model was greater than that in the small model. For example, the reinforcement pull-out with a displacement of 4 δ_y, which was close to the ultimate displacement was 0.4 ϕ in the large model, three times greater than that of the small model (0.13 ϕ) when converted into a non-dimensional reinforcement diameter. This is considered attributable to a decrease in bond strength between reinforcement and concrete due to the close spacing of reinforcement and its multi-layered arrangement in the large model.

③ Analysis was conducted on the large model with multi-layered reinforcement details to investigate the main reinforcement pull-out induced by reversed cyclic loading using the τ - s model proposed by Suzuki et al. It was found that the model was not quite satisfactorily able to predict the behavior of the large model. Therefore, instead of this model, a modified τ - s model reflecting the influence of the close reinforcement spacing was developed and used for the same analysis. And then, the result revealed that the modified τ - s model is able to simulate relatively satisfactorily the measured amount of reinforcement pull-out and distribution of reinforcement strain inside the footings.

④ As a simulation, nonlinear RC analysis taking into account reinforcement pull-out using a nonlinear rotation spring was carried out on the experimental results utilizing a fiber model. The results verify that the load-displacement relationship obtained in the experiment was predicted well by this analytical method.

Acknowledgements

The authors greatly appreciate the valuable advice from members of the Hanshin Expressway's 'Technical Research Group for Investigating the Ductility of RC Piers' in completing this paper.

References

[1] Akimoto and Osaka "Study on the Deformation Capacity of RC Piers under Seismic Loading," Proc. of the Colloquium on the Ductility of Concrete Structures and its Evaluation, pp. II-241-252, 1988.3 (in Japanese)
[2] Kawashima, K., Unjoh, S., Sugita, and Nakajima "Study on Main Reinforcement Cut-Off of the RC Bridge Piers under Seismic Loading, Evaluation of Seismic Resistivity and Reinforcing Methods," Technical Report of PWRI of the Ministry of Construction, Vol. 189, p. 96, 1993.9 (in Japanese)
[3] Ishibashi, T., and Yoshino, S. "Study on Deformation Capacity of Reinforced Concrete Bridge Piers Under Earthquake," Proc. of JSCE No. 390, V-8, pp. 57-66, 1988.2 (in Japanese)
[4] Ozaka, Y., Suzuki, M., Kuwasawa, S., and Ishibashi, T. "Load-Deflection Characteristics of Reinforced Concrete Columns Under Static Alternating Cyclic Loads," Proc. of JSCE No. 372, V -5, pp. 45-54, 1986.8 (in Japanese)
[5] Machida, A., Mutuyoshi, H., and Toyoda, K. "Evaluation of the Ductility of Reinforced Concrete Members," Proc. of JSCE No.378, V-6, pp.203-212, 1987. 2 (in Japanese)
[6] Suzuki, M., Jang, I., Watanuki, M., and Ozaka, Y. "Study on the Pullout Property of Axial Bars from Footings," Proc. of Concrete Research and Technology, JCI, Vol.3, No.1, pp. 33-44, 1992 (in Japanese)
[7] *Design Procedures for Reinforced Concrete Structures,* Hanshin Expressway Public Corporation, 1991.4 (in Japanese)
[8] Murayama, Y., Suda, K., and Mimura. "Effect of Column Reinforcement Pull Out on the Deformation Capacity of RC Piers," Proc. of the Colloquium on the Ductility of Concrete Structures and its Evaluation, 1988.3 (in Japanese)
[9] Yamamoto, T., Ishibashi, T, Otsubo, M., and Kobayashi, S. "Experimental Studies on Seismic Resistance of a Pier with Reinforcement Terminated in a Tension Zone," Proc. of JSCE, No. 348, V-1, pp. 61-70, 1984.8 (in Japanese)
[10] Yamada, Y., Iemura, H., Matumoto, T., Riestic, D., and Ukon, H.
"Stress-Strain Based Inelastic Earthquake Response Analysis of Reinforced Concrete Frame Structures," Proc. of IABSE International Symposium, Delft, 1987
[11] Muguruma, H., Watanabe, F., Iwashimizu, T., and Mitueda, R. "Ductility Improvement of High-Strength Concrete by Lateral Confinement," Transactions of Japan Concrete Institute, Vol. 5, pp. 403-410, 1988
[12] Menengotto, M., and Pinto, P. "Method of Analysis for Cyclically Loaded Reinforced Concrete Plane Frames Including Changes in Geometry and Nonelastic Behavior of Elements under Combined Normal Force and Bending," IABSE Symposium on Resistance and Ultimate Deformability of Structures Acted on by Well-Defined Repeated Loads, Final Report, Lisbon, 1973